

Aerila image analysis with generative adversarial networks

Joar Gruneau
joar@gruneau.se

March 9, 2018

1 Abstract

2 Introduction

Convolutional neural networks (CNN) have had great success for computer vision tasks [29, 44, 31, 14]. The success is possible thanks to graphical processing units (GPUs) and large scale human annotated datasets which the networks can learn from. CNN have progressed from single object detection in images [13] to multiple object detection and bounding box prediction [17]. CNN networks have also had great success in different segmentation task [5]. There is a similar trend in segmentation where we are moving from the easier task of semantic segmentation to the more complex task of instance segmentation. In semantic segmentation every pixel is mapped to a class and in instance segmentation the different instances of objects are separated detected for each class. Much work has gone into constructing well suited loss functions for segmentation [27, 42, 22]. Often the loss function fails to enforce important properties such as spatial contiguity in the segmentation maps [18] or proper spatial separation [3]. Conditional markov random fields (CRFs) have been a popular post processing step to ensure spatial contiguity in segmentation maps [45].

A new popular network for image to image translations are generative adversarial networks. The network consists of a generator network which performs the image translation and a discriminative network which aims to learn the loss function to differentiate the generated samples from the ground truth ones [7]. These type of networks have had great success on image to image translation tasks and are able to produce much more artistically pleasing mappings then networks without the adversarial loss [15, 12]. The success comes from the general approach where the network can learn it's own loss function which has proven beneficial for many tasks where a effective loss function is hard to express simply.

GANs have also been applied to image segmentation and has shown to give an increased performance [18, 34]. GANs have proven to be especially successful on small dataset such as medical segmentation where the human annotations usually are costly due to the required medical expertise needed to create correct annotations [34, 39, 41, 26, 1].

Analysis of aerial images can be a useful tool to obtain real time data cost effectively [??]. To mention a few applications it can be used to monitor traffic flow, construction progress, forest felling, water reserve capacity and to obtain accurate data for new maps. It can also be used to predict market trends since if we continuously can count the number of vehicles outside a marketplace we can more accurately predict how many customers that are

visiting the marketplace and therefore make more accurate predictions about the markets earnings.

However detecting and counting objects in aerial images has proven to be a troublesome area [??]. The objects of interest are usually very small compared to the image and there can be many objects in the same image. This causes naive classification networks to achieve bad performance if the entire image is fed in at once. To combat this some form of segmentation is usually done and the image is fed into the network in patches. Earlier methods fed explicit image patches through the CNN [11]. This achieved good performance but at a great computational cost since redundant computation of low-level filters for overlapping patches had to be performed [18]. To combat this different forms of segmentation algorithms were used such as the mean-shift-algorithm which drastically decreased the number of patches which had to be fed through the network [?]. The next step is instant segmentation of images where every pixel i CNN aerial images [3, 11, 47]

3 Relevant Theory

3.1 Generative adversarial networks

Goodfellow *et al* [7] first proposed the generative adversarial network (GAN). The network consists of two parts, a generator and a discriminator. The generators task is to generate samples from some data distribution. The discriminators task is to differentiate these generated samples from the true samples. This results in a counter fitting game where the generator continuously tries to produce better generated data to fool the discriminator and the discriminator is forced to become better at differentiating these generated samples from the true samples.

A common solution to try to force the generator to generate samples from the entire distribution is to input a noise vector into the generator [24]. Since we in this work are only interested in segmentation where a deterministic mapping from the image to the segmentation map is desired we will not input any noise vector into the generator.

3.1.1 Unconditional generative adversarial networks

Unconditional GANs are the simplest form of GANs. Here the discriminator does not observe the input to the generator. This means that the discriminator will learn a loss function which does not depend on the generators input [12]. We first define the binary cross entropy loss.

$$\ell_{bce}(\hat{z}, z) = -(z \ln(\hat{z}) + (1 - z) \ln(1 - \hat{z})) \quad (1)$$

Here \hat{z} is the prediction and z is the ground truth. The loss function for a unconditional GAN can then be described as.

$$\mathcal{L}(G, D) = -(\ell_{bce}(D(y), 1) + \ell_{bce}(D(G(x)), 0)) \quad (2)$$

Here D stands for the discriminating network and G for the generating network. G tries to minimize this function and D tries to maximize it. Hence we get a minimax game

$$G^* = \operatorname{argmin}_G [\max_D [\mathcal{L}(G, D)]] \quad (3)$$

3.1.2 Conditional generative adversarial networks

A conditional generative adversarial network (cGAN) was proposed by [19]. By letting the discriminator observe the input to the generator we can condition the loss function the discriminator learns on this input. This is of great importance here since we are not just trying to generate any semantic maps but semantic maps corresponding to the input image. The objective function will in this case be given by and the networks is trained with the minimax equation (3).

$$\mathcal{L}(G, D) = -(\ell_{bce}(D(x, y), 1) + \ell_{bce}(D(x, G(x)), 0)) \quad (4)$$

It has been shown that a multi term loss function can improve the quality of the generator [20, 12]. For image to image mappings a \mathcal{L}_1 or \mathcal{L}_2 loss is usually used. However for multi class image segmentation a multi class cross entropy loss is a better option to enforce the generator to assign a high probability to the correct class. The multi class cross entropy loss is given below.

$$\ell_{mce}(\hat{y}, y) = - \sum_{n=1}^{H*W} \sum_{n=1}^C y * \log(\hat{y}) \quad (5)$$

Here y is the ground truth segmentation maps while \hat{y} is the predicted maps. The discriminators objective is unchanged but the generator now has to fool the discriminator as well as minimizing the distance to the ground truth.

$$G^* = \operatorname{argmin}_G [\max_D [\mathcal{L}(G, D)] + \lambda \ell_{mce}(G)] \quad (6)$$

Here λ is just a constant which controls the importance of the second loss term.

3.2 Segmentor networks

For the generative part of a gan a segmentor network is needed. This network takes a image as an input and produces segmentation maps. A fully convolotional network (FCN) was first proposed Shelhamer and Long *et al*

[30]. A FCN is a CNN without any fully connected layers. A network with fully connected layers must have a specific input size on the image while a FCN network can take inputs of any size. The key insight is that by the authors were that fully connected layers can be viewed as convolutions with kernels that cover their entire input region. Hence a CNN with fully connected layers can be viewed as a FCN since it takes patches from a image of any size and outputs a spatial output map when the patches are aggregated. While the resulting maps are equivalent the computational cost for the FCN is greatly reduced. This is because no overlapping regions between patches has to be computed. This makes these networks ideal for generating dense output maps such as for image segmentation

Ronneberger *et al* [27] builds on the advancements of the FCN to propose a new type of segmentation network. The U-NET uses a encoder decoder structure with skip connections from bottleneck layers to upsampled layers. These skip connections are crucial to segmentation tasks as the initial feature maps maintain low-level features such that can be properly exploited for accurate segmentation. The network has been shown to produce high accuracy results even on small sized datasets [33, 27, 12, 38, 40]. Ronneberger *et al* [27] attributes this to the networks structure which creates internal data augmentation.

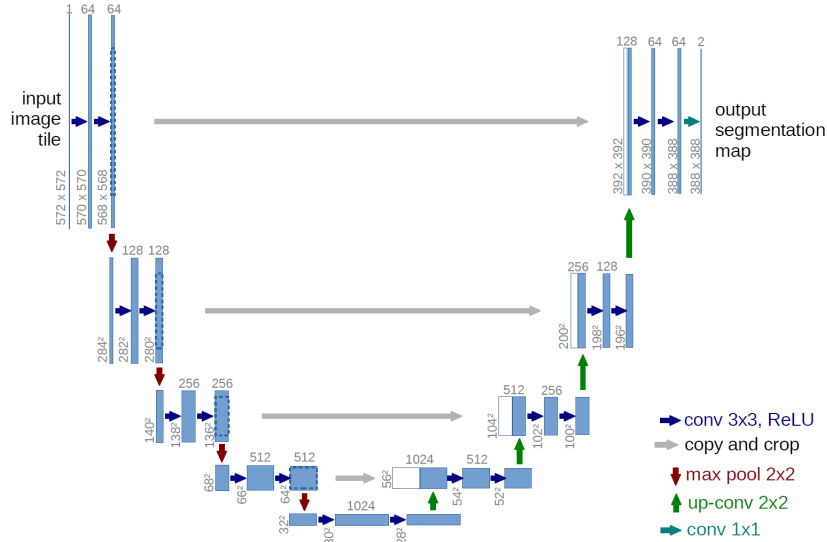


Figure 1: The initial u-net architecture proposed by Ronneberger *et al* [27]

Note that the size of the input image and the output prediction in 1 is different. This is because the u-net uses unpadding convolutions so at every convolutional layer one pixel is lost at every side. To obtain predictions in the borders of an image the the context is extrapolated by mirroring the

image [16]. It is also important that we choose an initial image size so the activation maps length is even through all layers of the network. [27]. In theory the u-net can handle images of any size but in practice we have memory limitations for the GPU. Segmentation is therefore done on patches and the output prediction can be directly stitched together without any overlapping.

3.3 Classification networks

For the discriminative part of the GAN a classification network is needed. This takes a input image and a set of segmentation maps and decides if the segmentation maps are artificial or ground truth. There are several high performing classification networks such as the VGG networks [32] and the ResNet networks [9].

The VGG networks in form of the sixteen layer VGG16 or the 19 layer VGG19 have performed very well on a wide variety of tasks such as classification [32]. They have been used inside Fast Region-based Convolutional Networks (fast R-CNN) [25, 6] to generate object activation maps for the regional proposal network (RPN). Fast R-CNN have been able to do object detection and bounding box prediction at a fraction of the time of earlier networks. They have also been used as a encoder in the SegNet architecture which has been a very popular segmentation network [4]. The

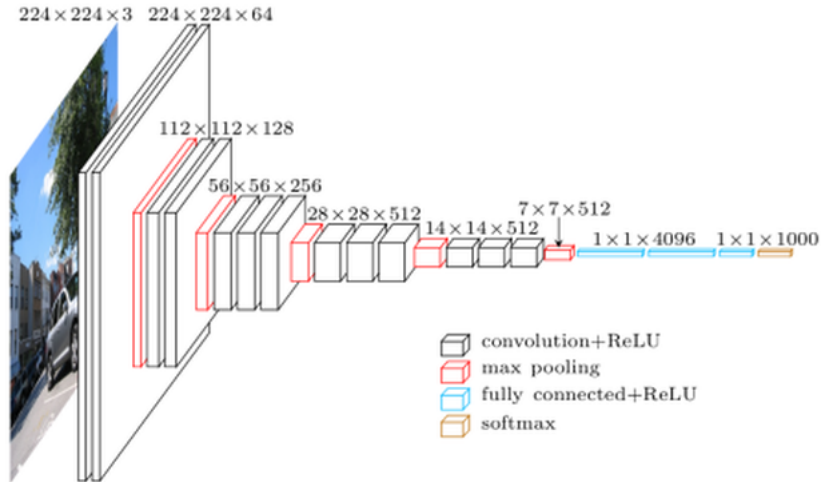


Figure 2: The VGG16 architecture proposed by [32]

VGG16 network takes inputs of images with size 224×224 and produces a class wise prediction. The network is very simple yet powerful and uses only 3×3 convolutions and 2×2 max pooling layers with stride 2.

ResNet is another widely popular classification network. It has performed very well on classification tasks [10, 36]. It has also been shown that wider residual networks are more memory efficient while still obtaining comparable performance [37, 43]. The success behind the ResNet lies in the residual

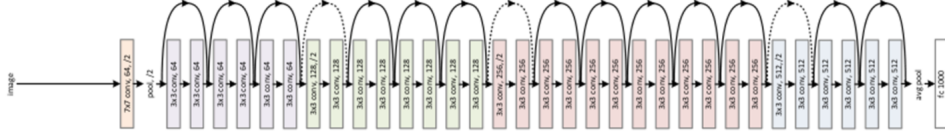


Figure 3: The 34 layer deep ResNet architecture [32]

blocks. A residual block is a two or more convolutional layers with a identity short-cut connection in between. The residual block can be defined as.

$$y = F(x, W) + x \quad (7)$$

The benefit of this is that this guarantees that the gradients will flow through the entire network. Therefore it is possible to build and train very deep residual networks by stacking hundreds of residual block. This also allows the network to itself decide the required depth since it can learn to set the weight of the final residual blocks to zero if they are not needed [9]. Hence we get a very flexible network where we easily can adapt the depth to the task at hand.

3.4 Dealing with severely imbalanced datasets

Due to the nature of aerial images the objects of interest are usually small compared to the entire image. This causes the dataset to be imbalanced since most pixels will belong to the background class. A naive segmentor could then obtain good accuracy by only predicting everything to the background class. To combat this there are several techniques. The most straight forward is to use a weighted cross entropy loss where every term is weighted depending on the class frequency [35]. Below is the weighted cross entropy loss for a two class segmentation problem.

$$\mathcal{L}_{wce} = -\omega * y * \log(\hat{y}) + (1 - y) \log(1 - \hat{y}) \quad (8)$$

Here y is the true probability for the foreground class \hat{y} the predicted probability for the foreground class and ω_c the class weights for the foreground class depending on the frequency. Another popular approach is to minimize the intersect over union loss [42, 22]

$$\mathcal{L}_{IoU} = 1 - \frac{\sum y \otimes \hat{y}}{\sum y + \sum \hat{y} - \sum y \otimes \hat{y}} \quad (9)$$

4 Related work

In most cases the segmentation networks needs some post processing to improve the accuracy of the segmentation maps. Conditional random markov fields CRF have been very successfully to enforce spatial contiguity in the output maps [2, 18]. There have been wor that used mean field inference expressed as a recurrent convolutional networks to do CRF like post processing [28, 46]. Luc *et al* [18] proposed a adversarial segmentation network to enforce higher order potentials without being limited to a single class. Instead on directly enforcing these higher order potentials in a CRF model as post processing the goal was to enforce them in the generator directly with adversarial training. This technique also has the benefit of lower complexity since at test time only the generator will be used.

The generators task was to produce segmentation maps for the C classes. One initial concern was that the discriminator would trivially be able to differentiate the generated segmentation maps from the ground truth by only examining if they were continuous or discrete. To combat this a scaling method was proposed where the ground truth segmentation maps were processed so that a mass of τ where placed on the correct label but were otherwise made as similar as possible to the generated maps (in regard to KL divergence). The scaling method showed no improvement over the basic method with no pre processing.

Son and Jung *et al* [33] showed that a U-NET combined with an adversarial loss could achieve state of the art performance for retinal vessel segmentation in fundoscopic images. The team investigated several types on adversarial networks proposed in [12] such as image-GAN, patch-GAN and pixel-GAN. For Image-GAN the discriminator make a decision on a image level if the image is generated or not. For patch-GAN the images are split into patches and the discriminator analyses each individually. The result is the aggregated result from all patches. For pixel-GAN the discriminator makes it decision on pixel per pixel level. The team found that a image-GAN togheter with a cross entropy term preformed the best and outperformed the non adversarial segmentor trained only with the cross entropy loss by a significant margin.

5 Network Architecture

For the generator network a U-NET will be used. The objective function for the GAN will be. Using the definition of the binary cross entropy loss (1) and the multi class cross entropy loss (5) we can now define our loss function

as.

$$\mathcal{L}(G, D) = \ell_{mce}(G(x), y) - \lambda(\ell_{bce}(D(x, y), 1) + \ell_{bce}(D(x, G(x)), 0)) \quad (10)$$

The generator will try to minimize this loss while the discriminator will try to maximize it. Following the example of [8, 18] and replace the term $-\lambda\ell_{bce}(D(G(x), y), 0)$ with $+\lambda\ell_{bce}(D(G(x), y), 1)$. Hence instead of minimizing the probability of the discriminative network to predict the generated map to be synthetic we maximize the probability of predicting the generated map as ground truth. The reason for this is that it leads a stronger gradient for the discriminator when making predictions on ground truth and generated maps. The binary cross entropy loss then becomes,

$$\mathcal{L}_{bce}(G, D) = \lambda(\ell_{bce}(D(x, G(x)), 1) - \ell_{bce}(D(x, y), 1)) \quad (11)$$

The objective for the network hence becomes.

$$G^* = \operatorname{argmin}_G[\max_D[\mathcal{L}_{bce}(G, D)] + \ell_{mce}(G(x), y)] \quad (12)$$

The generated segmentation maps will be concatenated with the image the basic manner since [18] did not gain any improvements with a product or scaling approach above the basic. Pinheiro *et al* [21] showed that it is preferable to have the same number of channels for each input to avoid that one input becomes dominating. Therefore the individual kernels will be applied to the image before concatenating them with the semantic maps. This also allows for a different low level representation of the image.

6 The dataset

6.1 The VEDAI dataset

The VEDAI dataset [23] consists of 9 different classes, these classes and the number of objects are given in the table below.

Classes	Number
Car	1340
Pick-up	950
Truck	300
Plane	47
Boat	170
Camping car	390
Tractor	190
Vans	100
Other	100

To make the results comparable with the extensive research of different methods done by [47] the classes plane, boat tractor van and other were removed due to scarcity of data. The annotations for each target consists on the centre coordinates of the target the angle of the center line of the bounding box as well as the corners of the bounding box. The bounding box fits the target closely so no extra information is given on the sides. The evaluation metrics on the VEDAI dataset are:

$$Precision = \frac{True\ positive}{True\ Positive + False\ poitive} \quad (13)$$

$$Recall = \frac{True\ positive}{True\ Positive + False\ negative} \quad (14)$$

$$F1\ score = \frac{2 * Recall * Precision}{Recall + Precision} \quad (15)$$

7 Related Work

References

- [1] A. Arbelle and T. R. Raviv. Microscopy Cell Segmentation via Adversarial Neural Networks. *arXiv:1709.05860 [cs]*, Sept. 2017. URL <http://arxiv.org/abs/1709.05860>. arXiv: 1709.05860.
- [2] A. Arnab, S. Jayasumana, S. Zheng, and P. Torr. Higher Order Conditional Random Fields in Deep Neural Networks. *arXiv:1511.08119 [cs]*, Nov. 2015. URL <http://arxiv.org/abs/1511.08119>. arXiv: 1511.08119.
- [3] N. Audebert, B. Le Saux, and S. Lefèvre. Segment-before-Detect: Vehicle Detection and Classification through Semantic Segmentation of Aerial Images. *Remote Sensing*, 9(4):368, Apr. 2017. doi: 10.3390/rs9040368. URL <http://www.mdpi.com/2072-4292/9/4/368>.
- [4] V. Badrinarayanan, A. Kendall, and R. Cipolla. SegNet: A Deep Convolutional Encoder-Decoder Architecture for Image Segmentation. *arXiv:1511.00561 [cs]*, Nov. 2015. URL <http://arxiv.org/abs/1511.00561>. arXiv: 1511.00561.
- [5] A. Garcia-Garcia, S. Orts-Escolano, S. Oprea, V. Villena-Martinez, and J. Garcia-Rodriguez. A Review on Deep Learning Techniques Applied to Semantic Segmentation. *arXiv:1704.06857 [cs]*, Apr. 2017. URL <http://arxiv.org/abs/1704.06857>. arXiv: 1704.06857.
- [6] R. Girshick. Fast R-CNN. *arXiv:1504.08083 [cs]*, Apr. 2015. URL <http://arxiv.org/abs/1504.08083>. arXiv: 1504.08083.

- [7] I. Goodfellow. NIPS 2016 Tutorial: Generative Adversarial Networks. *arXiv:1701.00160 [cs]*, Dec. 2016. URL <http://arxiv.org/abs/1701.00160>. arXiv: 1701.00160.
- [8] I. J. Goodfellow, J. Pouget-Abadie, M. Mirza, B. Xu, D. Warde-Farley, S. Ozair, A. Courville, and Y. Bengio. Generative Adversarial Networks. *arXiv:1406.2661 [cs, stat]*, June 2014. URL <http://arxiv.org/abs/1406.2661>. arXiv: 1406.2661.
- [9] K. He, X. Zhang, S. Ren, and J. Sun. Deep Residual Learning for Image Recognition. *arXiv:1512.03385 [cs]*, Dec. 2015. URL <http://arxiv.org/abs/1512.03385>. arXiv: 1512.03385.
- [10] K. He, X. Zhang, S. Ren, and J. Sun. Identity Mappings in Deep Residual Networks. *arXiv:1603.05027 [cs]*, Mar. 2016. URL <http://arxiv.org/abs/1603.05027>. arXiv: 1603.05027.
- [11] A. C. Holt, E. Y. W. Seto, T. Rivard, and P. Gong. Object-based detection and classification of Vehicles from high-resolution aerial photography. *Photogrammetric Engineering and Remote Sensing*, 75(7):871–880, July 2009. ISSN 0099-1112. URL <https://iths.pure.elsevier.com/en/publications/object-based-detection-and-classification-of-vehicles-from-high-r>.
- [12] P. Isola, J.-Y. Zhu, T. Zhou, and A. A. Efros. Image-to-Image Translation with Conditional Adversarial Networks. *arXiv:1611.07004 [cs]*, Nov. 2016. URL <http://arxiv.org/abs/1611.07004>. arXiv: 1611.07004.
- [13] A. Krizhevsky. Learning multiple layers of features from tiny images. Technical report, 2009.
- [14] A. Krizhevsky, I. Sutskever, and G. E. Hinton. ImageNet Classification with Deep Convolutional Neural Networks. In F. Pereira, C. J. C. Burges, L. Bottou, and K. Q. Weinberger, editors, *Advances in Neural Information Processing Systems 25*, pages 1097–1105. Curran Associates, Inc., 2012. URL <http://papers.nips.cc/paper/4824-imagenet-classification-with-deep-convolutional-neural-networks.pdf>.
- [15] C. Ledig, L. Theis, F. Huszar, J. Caballero, A. Cunningham, A. Acosta, A. Aitken, A. Tejani, J. Totz, Z. Wang, and W. Shi. Photo-Realistic Single Image Super-Resolution Using a Generative Adversarial Network. *arXiv:1609.04802 [cs, stat]*, Sept. 2016. URL <http://arxiv.org/abs/1609.04802>. arXiv: 1609.04802.

- [16] R. Li, W. Liu, L. Yang, S. Sun, W. Hu, F. Zhang, and W. Li. DeepUNet: A Deep Fully Convolutional Network for Pixel-level Sea-Land Segmentation. *arXiv:1709.00201 [cs]*, Sept. 2017. URL <http://arxiv.org/abs/1709.00201>. arXiv: 1709.00201.
- [17] T.-Y. Lin, M. Maire, S. Belongie, L. Bourdev, R. Girshick, J. Hays, P. Perona, D. Ramanan, C. L. Zitnick, and P. Dollár. Microsoft COCO: Common Objects in Context. *arXiv:1405.0312 [cs]*, May 2014. URL <http://arxiv.org/abs/1405.0312>. arXiv: 1405.0312.
- [18] P. Luc, C. Couprie, S. Chintala, and J. Verbeek. Semantic Segmentation using Adversarial Networks. *arXiv:1611.08408 [cs]*, Nov. 2016. URL <http://arxiv.org/abs/1611.08408>. arXiv: 1611.08408.
- [19] M. Mirza and S. Osindero. Conditional Generative Adversarial Nets. *arXiv:1411.1784 [cs, stat]*, Nov. 2014. URL <http://arxiv.org/abs/1411.1784>. arXiv: 1411.1784.
- [20] D. Pathak, P. Krahenbuhl, J. Donahue, T. Darrell, and A. A. Efros. Context Encoders: Feature Learning by Inpainting. *arXiv:1604.07379 [cs]*, Apr. 2016. URL <http://arxiv.org/abs/1604.07379>. arXiv: 1604.07379.
- [21] P. O. Pinheiro, T.-Y. Lin, R. Collobert, and P. Dollár. Learning to Refine Object Segments. *arXiv:1603.08695 [cs]*, Mar. 2016. URL <http://arxiv.org/abs/1603.08695>. arXiv: 1603.08695.
- [22] M. A. Rahman and Y. Wang. Optimizing Intersection-Over-Union in Deep Neural Networks for Image Segmentation. In G. Bebis, R. Boyle, B. Parvin, D. Koracin, F. Porikli, S. Skaff, A. Entezari, J. Min, D. Iwai, A. Sadagic, C. Scheidegger, and T. Isenberg, editors, *Advances in Visual Computing*, pages 234–244, Cham, 2016. Springer International Publishing. ISBN 978-3-319-50835-1.
- [23] S. Razakarivony and F. Jurie. Vehicle Detection in Aerial Imagery : A small target detection benchmark. *Journal of Visual Communication and Image Representation, Elsevier*, Mar. 2015. URL <https://hal.archives-ouvertes.fr/hal-01122605>.
- [24] S. Reed, Z. Akata, X. Yan, L. Logeswaran, B. Schiele, and H. Lee. Generative Adversarial Text to Image Synthesis. May 2016. URL <https://arxiv.org/abs/1605.05396>.
- [25] S. Ren, K. He, R. Girshick, and J. Sun. Faster R-CNN: Towards Real-Time Object Detection with Region Proposal Networks. *arXiv:1506.01497 [cs]*, June 2015. URL <http://arxiv.org/abs/1506.01497>. arXiv: 1506.01497.

- [26] M. Rezaei, K. Harmuth, W. Gierke, T. Kellermeier, M. Fischer, H. Yang, and C. Meinel. Conditional Adversarial Network for Semantic Segmentation of Brain Tumor. *arXiv:1708.05227 [cs]*, Aug. 2017. URL <http://arxiv.org/abs/1708.05227>. arXiv: 1708.05227.
- [27] O. Ronneberger, P. Fischer, and T. Brox. U-Net: Convolutional Networks for Biomedical Image Segmentation. *arXiv:1505.04597 [cs]*, May 2015. URL <http://arxiv.org/abs/1505.04597>. arXiv: 1505.04597.
- [28] A. G. Schwing and R. Urtasun. Fully Connected Deep Structured Networks. *arXiv:1503.02351 [cs]*, Mar. 2015. URL <http://arxiv.org/abs/1503.02351>. arXiv: 1503.02351.
- [29] P. Sermanet, D. Eigen, X. Zhang, M. Mathieu, R. Fergus, and Y. LeCun. OverFeat: Integrated Recognition, Localization and Detection using Convolutional Networks. *arXiv:1312.6229 [cs]*, Dec. 2013. URL <http://arxiv.org/abs/1312.6229>. arXiv: 1312.6229.
- [30] E. Shelhamer, J. Long, and T. Darrell. Fully Convolutional Networks for Semantic Segmentation. *arXiv:1605.06211 [cs]*, May 2016. URL <http://arxiv.org/abs/1605.06211>. arXiv: 1605.06211.
- [31] K. Simonyan and A. Zisserman. Two-Stream Convolutional Networks for Action Recognition in Videos. *arXiv:1406.2199 [cs]*, June 2014. URL <http://arxiv.org/abs/1406.2199>. arXiv: 1406.2199.
- [32] K. Simonyan and A. Zisserman. Very Deep Convolutional Networks for Large-Scale Image Recognition. *arXiv:1409.1556 [cs]*, Sept. 2014. URL <http://arxiv.org/abs/1409.1556>. arXiv: 1409.1556.
- [33] J. Son, S. J. Park, and K.-H. Jung. Retinal Vessel Segmentation in Fundoscopic Images with Generative Adversarial Networks. *arXiv:1706.09318 [cs]*, June 2017. URL <http://arxiv.org/abs/1706.09318>. arXiv: 1706.09318.
- [34] N. Souly, C. Spampinato, and M. Shah. Semi and Weakly Supervised Semantic Segmentation Using Generative Adversarial Network. *arXiv:1703.09695 [cs]*, Mar. 2017. URL <http://arxiv.org/abs/1703.09695>. arXiv: 1703.09695.
- [35] C. H. Sudre, W. Li, T. Vercauteren, S. Ourselin, and M. J. Cardoso. Generalised Dice overlap as a deep learning loss function for highly unbalanced segmentations. *arXiv:1707.03237 [cs]*, 10553:240–248, 2017. doi: 10.1007/978-3-319-67558-9_28. URL <http://arxiv.org/abs/1707.03237>. arXiv: 1707.03237.

- [36] C. Szegedy, S. Ioffe, V. Vanhoucke, and A. Alemi. Inception-v4, Inception-ResNet and the Impact of Residual Connections on Learning. *arXiv:1602.07261 [cs]*, Feb. 2016. URL <http://arxiv.org/abs/1602.07261>. arXiv: 1602.07261.
- [37] Z. Wu, C. Shen, and A. v. d. Hengel. Wider or Deeper: Revisiting the ResNet Model for Visual Recognition. *arXiv:1611.10080 [cs]*, Nov. 2016. URL <http://arxiv.org/abs/1611.10080>. arXiv: 1611.10080.
- [38] Y. Xue, T. Xu, H. Zhang, R. Long, and X. Huang. SegAN: Adversarial Network with Multi-scale L_1 Loss for Medical Image Segmentation. *arXiv:1706.01805 [cs]*, June 2017. URL <http://arxiv.org/abs/1706.01805>. arXiv: 1706.01805.
- [39] Y. Xue, T. Xu, H. Zhang, R. Long, and X. Huang. SegAN: Adversarial Network with Multi-scale L_1 Loss for Medical Image Segmentation. *arXiv:1706.01805 [cs]*, June 2017. URL <http://arxiv.org/abs/1706.01805>. arXiv: 1706.01805.
- [40] D. Yang, D. Xu, S. K. Zhou, B. Georgescu, M. Chen, S. Grbic, D. Metaxas, and D. Comaniciu. Automatic Liver Segmentation Using an Adversarial Image-to-Image Network. *arXiv:1707.08037 [cs]*, July 2017. URL <http://arxiv.org/abs/1707.08037>. arXiv: 1707.08037.
- [41] D. Yang, D. Xu, S. K. Zhou, B. Georgescu, M. Chen, S. Grbic, D. Metaxas, and D. Comaniciu. Automatic Liver Segmentation Using an Adversarial Image-to-Image Network. *arXiv:1707.08037 [cs]*, July 2017. URL <http://arxiv.org/abs/1707.08037>. arXiv: 1707.08037.
- [42] J. Yu, Y. Jiang, Z. Wang, Z. Cao, and T. Huang. UnitBox: An Advanced Object Detection Network. *arXiv:1608.01471 [cs]*, pages 516–520, 2016. doi: 10.1145/2964284.2967274. URL <http://arxiv.org/abs/1608.01471>. arXiv: 1608.01471.
- [43] S. Zagoruyko and N. Komodakis. Wide Residual Networks. *arXiv:1605.07146 [cs]*, May 2016. URL <http://arxiv.org/abs/1605.07146>. arXiv: 1605.07146.
- [44] M. D. Zeiler and R. Fergus. Visualizing and Understanding Convolutional Networks. *arXiv:1311.2901 [cs]*, Nov. 2013. URL <http://arxiv.org/abs/1311.2901>. arXiv: 1311.2901.
- [45] Y. Zhao, L. Zhang, P. Li, and B. Huang. Classification of High Spatial Resolution Imagery Using Improved Gaussian Markov Random-Field-Based Texture Features. *IEEE Transactions on Geoscience and Remote Sensing*, 45(5):1458–1468, May 2007. ISSN 0196-2892. doi: 10.1109/TGRS.2007.892602.

- [46] S. Zheng, S. Jayasumana, B. Romera-Paredes, V. Vineet, Z. Su, D. Du, C. Huang, and P. H. S. Torr. Conditional Random Fields as Recurrent Neural Networks. *arXiv:1502.03240 [cs]*, pages 1529–1537, Dec. 2015. doi: 10.1109/ICCV.2015.179. URL <http://arxiv.org/abs/1502.03240>. arXiv: 1502.03240.
- [47] J. Zhong, T. Lei, and G. Yao. Robust Vehicle Detection in Aerial Images Based on Cascaded Convolutional Neural Networks. *Sensors (Basel, Switzerland)*, 17(12), Nov. 2017. ISSN 1424-8220. doi: 10.3390/s17122720. URL <https://www.ncbi.nlm.nih.gov/pmc/articles/PMC5751529/>.